

Depth imaging of elastic wavefields - Where P meets S

Brian H. Hoffe and Laurence R. Lines

ABSTRACT

The multicomponent recording of reflected elastic wavefields allows for an analysis of compressional and shear wave velocities. For seismic arrivals initiated by dynamite sources and reflected from a layered sedimentary system, it is natural to consider both P and P-S reflections as recorded on vertical and in-line components of the geophones. Since P-wave and S-wave velocities will differ (roughly by a factor of 2), it is an interpretative art to correlate the P-wave reflections with P-S reflections. In an attempt to correlate or “tie” these reflections, time sections are often stretched and squeezed to match reflection positions. However, the domain in which these reflectors should naturally tie is the depth domain. Depth images for the P-P and P-S reflections can be obtained using depth migration. We illustrate this method of reflector imaging via poststack depth migration “where P meets S” on a data set from the Blackfoot field.

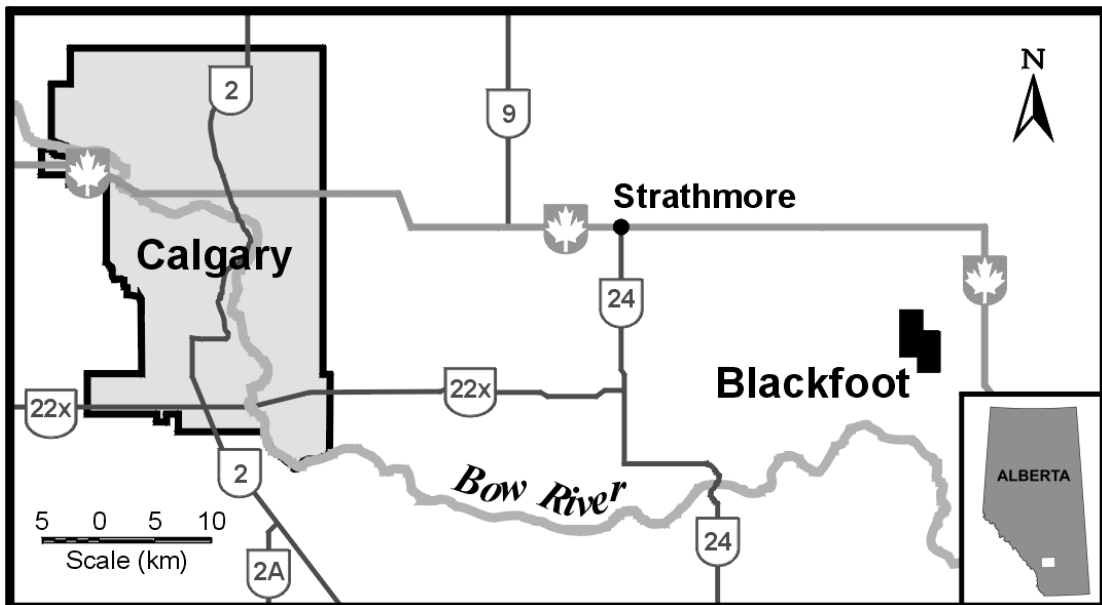


Figure 1. Map showing the location of the Blackfoot field where the high-resolution 3C-2D seismic survey was acquired.

The processed P-P and P-S structure stacks for the 20 m receiver interval data were depth migrated via a reverse-time algorithm using P and S velocities measured in a well directly adjacent to the seismic profile. These depth migrated sections show good correlation over the well interval where velocities were measured. Thus migration of both vertical and converted wave stacked data to the depth domain may provide a much better means of correlation than the current practice of correlating in time which is rather cumbersome and degrades the quality of the data being compared.

INTRODUCTION

On November 1 - 2, 1997 the CREWES Project at the University of Calgary with assistance from Boyd PetroSearch Consultants Ltd. and PanCanadian Petroleum Ltd. recorded a unique, high-resolution 3C-2D seismic survey at the PanCanadian-owned Blackfoot field. The Blackfoot field is located some 50 - 55 km east of Calgary near the town of Strathmore, Alberta (Figure 1). The producing formation within the Blackfoot area is a Lower Cretaceous, cemented glauconitic sand which was deposited as incised channel-fill sediment above the Mississippian carbonates (Wood and Hopkins, 1992). The Glauconitic sandstone lies at depth of about 1,500 m below surface and is up to 45 m thick. The average porosity in this producing sandstone is near 18% and the cumulative production from it throughout southern Alberta exceeds 200 MMbbls oil and 400 BCF gas (Miller et al., 1995).

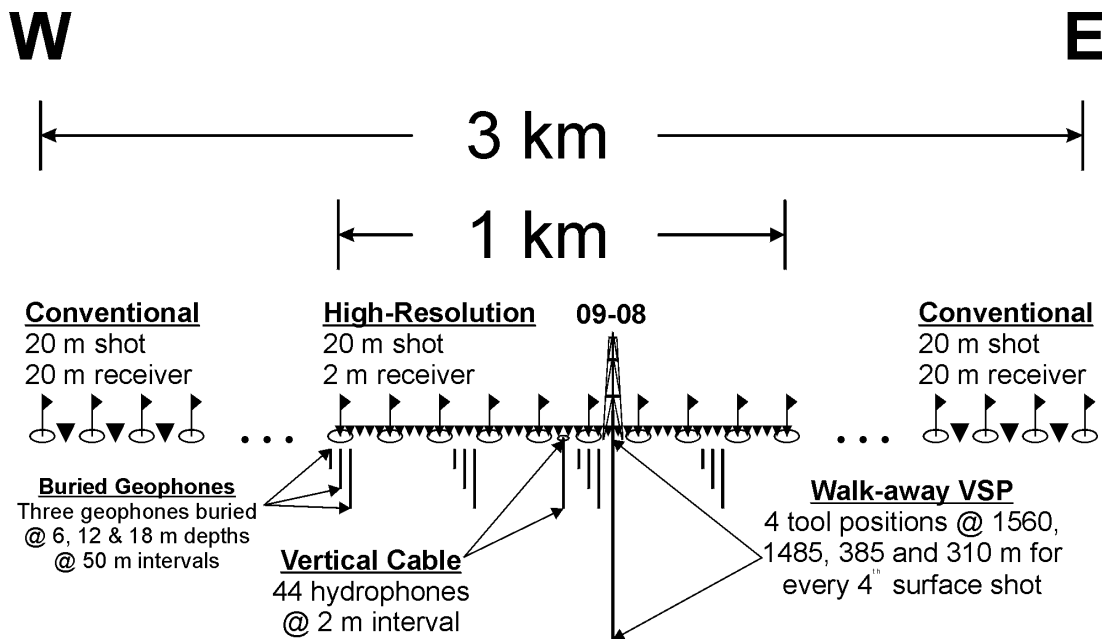


Figure 2. Schematic diagram (not to scale) illustrating the layout of the Blackfoot 3C-2D high-resolution seismic survey.

The survey involved the acquisition of a 3 km 3C-2D reflection profile which consisted of a combination of conventional and high-resolution receiver intervals. A schematic diagram of the survey is presented in Figure 2. The source interval employed for the entire 2D profile was 20 m shot on the half-station. However, the receiver interval changed from 20 m to 2 m in the central part of the profile. The survey also involved simultaneous recording into 21×3 buried 3-C geophones situated in 6, 12 and 18 m holes drilled every 50 m along the central km of the profile. In addition to these buried geophones, a 48-channel vertical hydrophone cable with a 2 m receiver interval was deployed in a 100 m cased hole located in the centre of the profile. A walk-away VSP was also simultaneously recorded in PanCanadian's 100/09-08-23-23W4 well located near the centre of the spread by recording the full range of offsets for each tool position.

Interest in multicomponent seismic data is a result of our ability to discriminate lithology more accurately based on both P (compressional) and S (shear) wave information, rather than by using P-wave data alone. An excellent example of lithologic discrimination by use of P-wave and S-wave data was shown in the case history from the Lambert field, Colorado, given by Ruckgaber (1990). In this case history, the inversion for P-wave and S-wave velocities allowed for the accurate discrimination between sandstones and shales in the subsurface. This seismic lithologic discrimination was later confirmed by the use of gamma ray logs acquired from wells within the Lambert field. Although this excellent project effectively showed the advantage of using both P-wave and S-wave impedance estimates, P-wave time sections were compared to S-wave sections by compressing S-wave travel times using ratios of P to S isochrons between principal reflectors. One can imagine many rock types where such a time conversion would be difficult.

1. **Geometry, Trace Kills & Reversals**
2. **Surface-Consistent Deconvolution + TV Whitening**
3. **Refraction Statics + Surface Consistent Statics**
4. **NMO**
5. **TV Scaling**
6. **CDP Trim Statics**
7. **CDP Stack**
8. **Trace Equalization**

Table 1. Processing sequence used to produce the P-P structure stack.

1. **Geometry, Trace Kills & Reversals**
2. **Surface-Consistent Deconvolution + TV Whitening**
3. **Vertical Component Statics + Residual Receiver Statics**
4. **Surface Consistent Statics**
5. **Converted Wave NMO**
6. **TV Scaling**
7. **ACP Trim Statics**
8. **Converted Wave Stack**
9. **Trace Equalization**

Table 2. Processing sequence used to produce the P-S structure stack.

Therefore, we propose a different strategy for matching elastic wavefields which utilizes depth migration. The strategy is based on the fact that P and S reflected wavefields emanate from the same reflectors at depth. Therefore, if we are to depth migrate the wavefields with accurate velocity estimates, we should correctly image reflectors in depth on both P-P and P-S sections. We demonstrate this by using a data example from the recently acquired Blackfoot 3C-2D high-resolution survey described above. For these multicomponent data, we will deal with comparisons of the "quasi-P" section with the predominantly "P-S" section.

METHODOLOGY

The Blackfoot high-resolution 3-C data was processed commercially by Matrix Geoservices Ltd. and we present only the results from the conventional, 20 m receiver interval data. The processing flow used to produce the P-P and P-S structure stacks

input into the migrations is presented in Tables 1 and 2 respectively. Unmigrated structure stacks from the Blackfoot field exhibit reflectors which are essentially horizontal displaying little to no structure. As previously mentioned, dynamite was used as a source which would generate a predominantly P down-going wavefield. Because a majority of the reflectors are flat-lying, reflected energy recorded on the in-line component would predominantly be P-S mode converted arrivals.

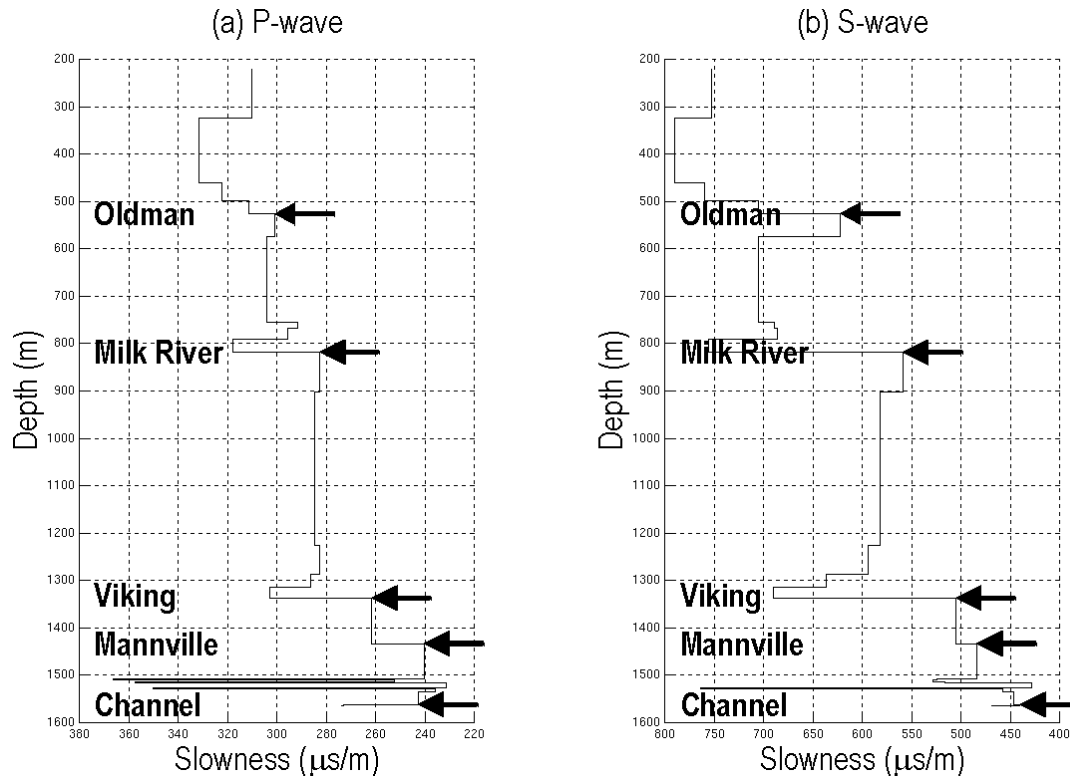


Figure 3. The formation-blocked (a) compressional and (b) shear wave sonic logs as measured in Pan-Canadian's 100/09-08-23-23W4 well located near the centre of the recording spread. These blocked logs were used to formulate the velocity functions used to migrate both P-P and P-S structure stacks.

P and S sonic velocities measured in the 09-08 well located adjacent to the seismic profile were used for the reverse-time depth migrations. The velocities were first blocked using the major formation tops to yield P and S interval velocity functions in depth. These blocked velocity logs are presented in Figure 3. In order to generate an interval velocity field for migration of the converted wave or P-S section, an average of the slowness for the P and S blocked logs was used.

Once a velocity-depth model has been established by blocking the logs, the mapping of time sections into depth sections can be achieved by reverse-time depth migration as described by McMechan (1983). For stacked data, the reverse-time depth migration effectively moves the time samples downward to their point of origin by using wave equation propagation. Since the reverse-time method is based on finite differencing of the wave equation, it can be effectively used for any elastic wavefield – provided we supply accurate interval velocities for the data sets. For migrating the stacked P-wave data, we use one-way wave propagation with $\frac{1}{2}$ of the P-wave

velocity. For migrating the stacked P-S data, we use one-way wave propagation with $\frac{1}{2}$ of a velocity whose slowness is the average of the P and S slowness values. Since we are dealing with predominantly vertically travelling energy, we use the P-wave and S-wave sonic logs to derive our interval velocities.

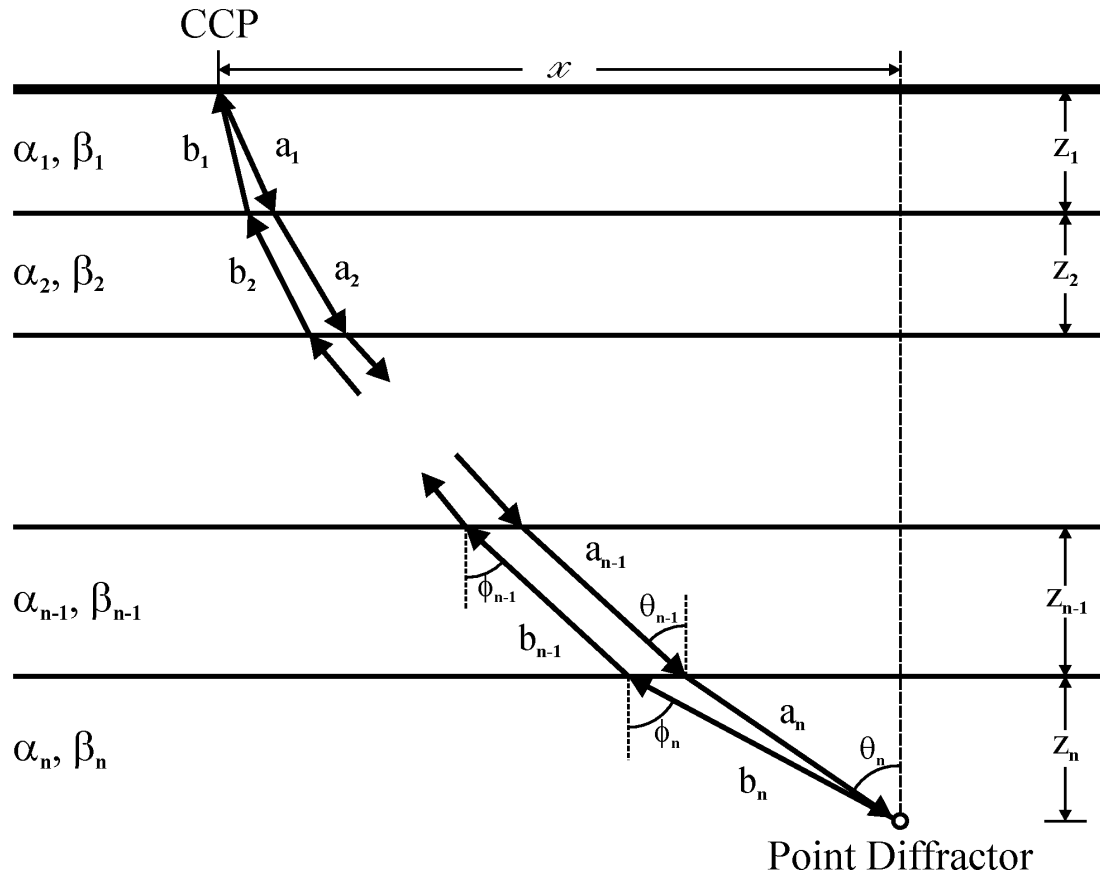


Figure 4. Zero-offset ray paths through a layered earth model from a point diffractor (after Harrison and Stewart, 1993).

The method that we have used in our reverse-time depth migration of converted wave data uses the assumption of an exploding reflector in which the P-S energy travels with a velocity given by the harmonic average of P-wave and S-wave velocities. Harrison and Stewart (1993) discuss poststack migration of P-S data and show that this model is only strictly correct if the V_p/V_s ratio is constant for all layers. Nevertheless, we show that the approximation of the P-S exploding reflector is valid for the velocity models that we use here in our migration. We validate the model by considering the zero-offset ray paths from a point diffractor through a layered earth whose velocities are given by the P-wave and S-wave logs, as shown by Figure 4. We also consider a ray path, generally between the P and S rays which represents the P-S exploding reflector ray path, and compare the travel time for these rays. That is we compare the travel time given by equation (1) (Harrison and Stewart, 1993):

$$t_{p+s} = \sum_{i=1}^n \frac{z_i}{\sqrt{1 - p_1^2 \alpha_i^2}} + \sum_{i=1}^n \frac{z_i}{\sqrt{1 - p_2^2 \beta_i^2}} \tag{1}$$

to the travel time given by equation (2):

$$t_{ps} = 2 \sum_{i=1}^n \frac{z_i}{\sqrt{1 - p_{12}^2 v_{mig}^2}} \tag{2}$$

where v_{mig} is the velocity derived by averaging the slownesses and p_{12} is the ray parameter for exploding reflector ray which gives the endpoints of the ray.

Table 3. Travel times as computed from equations (1) and (2) for a range of emergence angles.

Angle (radians)	t_{p+s} (s)	t_{ps} (s)	% Difference
0.0	1.49971	1.49971	0.000
0.1	1.51349	1.51347	0.001
0.2	1.55687	1.55677	0.006
0.3	1.63711	1.63677	0.020
0.4	1.77096	1.76980	0.065

Table 3 shows that for angles of emergence from 0.0 to 0.4 radians (approximately 0° to 23°) that the error from the P-S ray and the “exploding reflector ray” is less than the sampling interval of 1 ms for a 20 layer model. Hence, while Harrison and Stewart (1993) are correct in stating that the exploding reflector model is not strictly exact, it is a very good approximation for the situation that we are dealing with here.

In depth migrating these data, we should note that the velocity logs may not always supply the exact solution and, for some areas of the subsurface, logs are simply not available. In these areas where there is a need to adjust velocity, we can use the least-squares optimization approach proposed by Lines (1993), which adjusted interval velocities so that migrated depths matched the well information. In this case, we use the optimization method to adjust velocities so that the migrated P-P depths match those of the migrated P-S depths, in a least-squares sense.

CONCLUSIONS

The resultant depth-migrated P-P and P-S sections are presented in Figure 5. The P-wave and P-S reflected wavefields occur at different times on the vertical and in-line stacked sections from the Blackfoot field surveys. Rather than stretching and squeezing time sections to match reflectors, we utilize depth migration and interval velocities deduced from the logs to effectively define the reflector depths. Since reflections emanate from the reflecting beds at depth, the migrated sections show a good tie at depths of the major reflections. We also note that the depth migrated P-S section has similar or perhaps even better resolution (but not S/N levels) than the depth migrated P-P section.

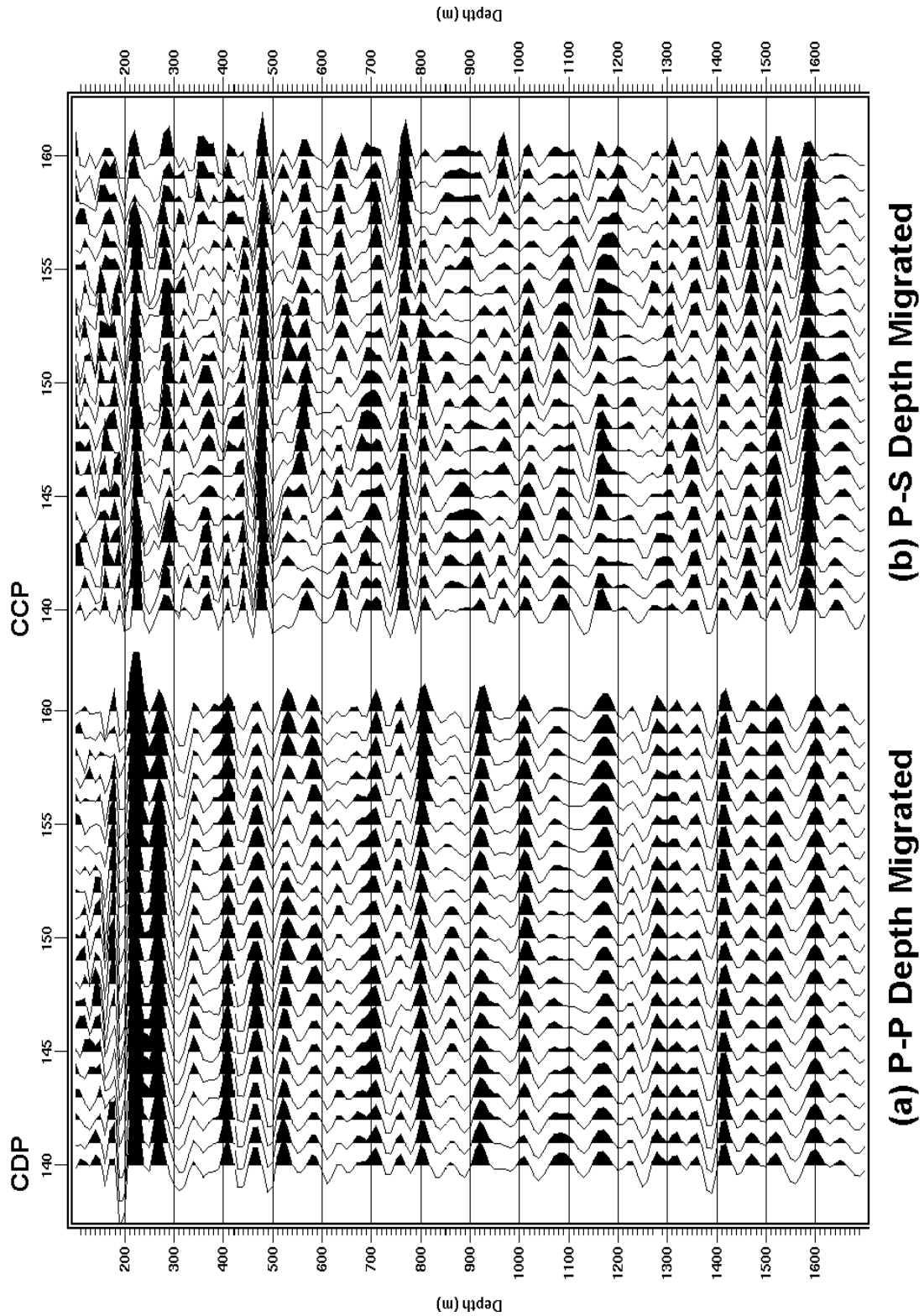


Figure 5. The reverse-time depth migrations for (a) the P-P and (b) P-S sections. These two sections exhibit good depth ties for the major reflectors contained within the well interval where the P and S sonic logs were recorded.

ACKNOWLEDGEMENTS

We would like to thank Mr. William Goodway and Mr. David Cooper of PanCanadian Petroleum Ltd. and Mr. John Boyd and Mr. Doug Eaton of Boyd PetroSearch for all their assistance in successfully acquiring this unique 3-C survey. We also thank Ms. Han-Xing Lu of the CREWES Project for her assistance in the preparation of the data used for the migrations.

REFERENCES

- Harrison, M. P. and Stewart, R.R. 1993. Poststack migration of P-SV seismic data. *Geophysics*, **58**, 1127-1135.
- Lines, L. 1993. Optimization of seismic migration through use of well information. *Canadian Journal of Exploration Geophysics*, Vol. **29**, No. **2**, 419-428.
- McMechan, G.A., 1983. Migration by extrapolation of time-dependent boundary values. *Geophysical Prospecting*, **31**, 413-420.
- Miller, S. L.M., Aydemir, E. O. and Margrave, G. F. 1995. Preliminary interpretation of P-P and P-S data from the Blackfoot broad-band survey. CREWES Project Research Report, **7**, Chapter 42.
- Ruckgaber, G.M., 1990. Seismic lithology estimation at Hambert Field, Colorado, U.S.A., preprint of paper presented at annual Norwegian Petroleum Institute Meeting.
- Wood, J. M. and Hopkins, J. C. 1992. Traps associated with paleovalleys and interfluves in an unconformity bounded sequence: Lower Cretaceous Glauconitic Member, southern Alberta, Canada. *AAPG Bull.* **76(6)**, 904-926.